

Spin Switching Effect in Nickel Nitroprusside: Design of a Molecular Spin Device Based on Spin Exchange Interaction

Z.-Z. Gu,[†] O. Sato,[‡] T. Iyoda,[‡] K. Hashimoto,^{*,†,‡} and A. Fujishima^{*,†}

Department of Applied Chemistry, The University of Tokyo, 7-3-1 Hongo Bunkyo-Ku, Tokyo 113, Japan, and Kanagawa Academy of Science and Technology, Tokyo Institute of Polytechnics, 1583 Iiyama, Atsugi, Kanagawa 243-02, Japan

Received December 16, 1996. Revised Manuscript Received February 19, 1997[®]

A new approach for designing optically switchable molecular communication devices based on spin-exchange interactions is proposed in the present paper. The device is constituted from two parts, i.e., a paramagnetic block (PMB) and a coupling control block (CCB). As a prototype of this model, nickel nitroprusside, $\text{Ni}[\text{Fe}(\text{CN})_5\text{NO}]\cdot 5.3\text{H}_2\text{O}$ was synthesized, in which the nickel ion acts as the PMB and the nitroprusside molecule does as the CCB. In this compound, as there is no spin on Fe, the magnetic interaction between the neighboring Ni cations is very weak. No magnetic phase transition can be observed until 1.8 K. Photoirradiation at 475 nm causes a charge transfer from the metal, Fe, to the ligand, NO, which induces two antiferromagnetically coupled spins on Fe and NO. Furthermore, the new spin on Fe interacts ferromagnetically with those on neighboring nicks. As a result, the spins on the Ni ions, which surround the Fe with spin, form a magnetic cluster with $S = 5$.

Introduction

Considerable attention has been attracted to the construction of novel molecular devices in the past few years,^{1–15} and this topic has been of long-term interest in our laboratory.^{6,11,12,14} Progress in designing molecular devices requires the establishment of a switchable communication link between different components and to the outside world. Until now, much of the effort has been devoted to establishing electronic communications using π -conjugated systems.^{8–10}

Recently a new research field, that of molecular-based magnets, has seen a boom in interest.^{12–14,16–21} Within this field, metal-spin-site-based magnets²² have held our

particular interest. In these materials, metal spin sites are usually bridged by a spacer moiety and a superexchange interaction couples the spin sites. Such coupling depends greatly on the properties of the spacer, which is usually composed of organic molecules. These can be prepared and modified by organic chemistry methodologies.²² The design of the photofunctionalized spacer allows us to control the magnetic coupling between spin sites by light irradiation. This approach provides an alternative method for the design of communication devices at a molecular level. In contrast to traditional electronic communication, a spin coupling is responsible for the molecular communication.

In this paper, we will report and analyze a spin switching effect found in nickel nitroprusside. This material can be regarded as a prototype for molecular spin devices.²³ It is also interesting from the viewpoint of magnetic recording materials, because it provides a method to design a novel photomagnetic material in which magnetic properties can be controlled by photoirradiation.

Model

A metal-spin-site-based magnet is usually composed of spin sites (in this paper denoted as paramagnetic blocks (PMB)) and spacers. A superexchange interac-

[†] The University of Tokyo.

[‡] Kanagawa Academy of Science and Technology.

* To whom correspondence should be addressed.

[®] Abstract published in *Advance ACS Abstracts*, April 1, 1997.

(1) Zhao, J.; Jurbergs, D.; Yamazi, B.; McDevitt, J. T. *J. Am. Chem. Soc.* **1992**, *114*, 2737–2738.

(2) Haupt, S. G.; Riley, D. R.; Jones, C. T.; Zhao, J.; McDevitt, J. T. *J. Am. Chem. Soc.* **1993**, *115*, 1196–1198.

(3) McDevitt, J. T.; Riley, D. R.; Haupt, S. G. *Anal. Chem.* **1993**, *65*, 535A–545A.

(4) Chen, K.; Mirkin, C. A. *J. Am. Chem. Soc.* **1995**, *117*, 6374–6375.

(5) Iwamoto, M.; Majima, Y.; Naruse, H.; Noguchi, T.; Fuwa, H. *Nature* **1991**, *353*, 645–647.

(6) Yao, J. N.; Hashimoto, K.; Fujishima, A. *Nature* **1992**, *355*, 624–626.

(7) Lindoy, L. F. *Nature* **1993**, *364*, 17–18.

(8) de Silva, A. P.; Gunaratne, H. Q. N.; McCoy, C. P. *Nature* **1993**, *364*, 42–44.

(9) Hush, N. S.; Wong, A. T.; Bacskay, G. B.; Reimers, J. R. *J. Am. Chem. Soc.* **1990**, *112*, 4192–4197.

(10) Benniston, A. C.; Goulle, V.; Harriman, A.; Lehn, J.-M.; Marczinke, B. *J. Phys. Chem.* **1994**, *98*, 7798–7804.

(11) Liu, Z. F.; Hashimoto, K.; Fujishima, A. *Nature* **1990**, *347*, 658.

(12) Sato, O.; Iyoda, T.; Fujishima, A.; Hashimoto, K. *Science* **1996**, *271*, 49–51.

(13) Verdager, M. *Science* **1996**, *272*, 698–699.

(14) Sato, O.; Iyoda, T.; Fujishima, A.; Hashimoto, K. *Science* **1996**, *272*, 704–705.

(15) Gu, Z.-Z.; Wu, H.; Wei, Y.; Liu, J. Z. *J. Phys. Chem.* **1993**, *97*, 2543–2545.

(16) Gatteschi, D.; Kahn, O.; Miller, J. S.; Palacio, F. *Magnetic Molecular Materials*; Kluwer: Dordrecht, Netherlands, 1991.

(17) Kahn, O. *Molecular Magnetism*; VCH: New York, 1993.

(18) Entley, W. R.; Girolami, G. S. *Science* **1995**, *268*, 397–400.

(19) Mallah, T.; Thiébaud, S.; Verdager, M.; Veillet, P. *Science* **1993**, *262*, 1554–1557.

(20) Kahn, O. *Nature* **1995**, *378*, 667–668.

(21) Ferlay, S.; Mallah, T.; Ouahès, R.; Veillet, P.; Verdager, M. *Nature* **1995**, *378*, 701–703.

(22) Miller, M. S.; Epstein, A. J. *Angew. Chem., Int. Ed. Engl.* **1994**, *33*, 385–415.

(23) Gu, Z.-Z.; Sato, O.; Iyoda, T.; Hashimoto, K.; Fujishima, A. *J. Phys. Chem.* **1996**, *100*, 18289–18291.

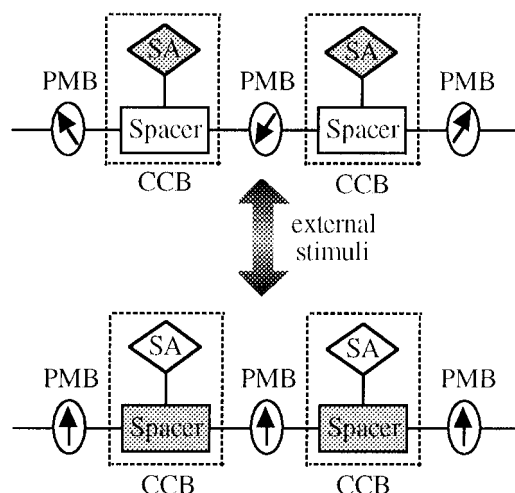


Figure 1. Model of a molecular spin device. A coupling control block (CCB) which is composed of a spacer and a spin acceptor (SA) is used to control the spin coupling between paramagnetic blocks (PMB) via external stimuli.

tion through the spacer couples the PMBs. Spin alignment in the PMBs is determined by the competition between the exchange interaction and thermal disordering. When the exchange interaction between spins dominates the thermal effects, the spins on the PMBs are ordered. Otherwise the spins are randomly oriented. As the exchange interaction depends greatly on the spacer, the alignment of the spins can be manipulated via control of the spacer. The type of spin device proposed here is schematically depicted in Figure 1. In this system, a coupling control block (CCB) is used instead of the conventional spacer to bridge the PMBs. A controllable spin acceptor (SA) is supplied to the CCB as a ligand. The state of the CCB can be changed via electron transfer between the spacer and the SA.

For the model system in Figure 1, there are two states, which can be switched by an external stimulus. In one state, the exchange interaction is well mediated by the CCB, and spins on neighboring sites are magnetically coupled. In the other state, the exchange interaction through the CCB is suppressed and spins on the PMBs are disordered.

In the present work, nickel nitroprusside is utilized to construct this model system, in which $\text{Fe}(\text{CN})_5\text{NO}^{2-}$ and Ni^{2+} act as the CCB and PMB, respectively. Since the nitrosyl group, utilized as the acceptor, has a relatively low unoccupied energy level, a metal-to-ligand charge transfer (MLCT) absorption band appears in the visible range. Thus, we can control the electronic and spin states of the compound via visible light illumination.

Experimental Section

Nickel nitroprusside was prepared by adding a 0.02 M aqueous solution of nickel chloride (Wako Chemicals) in slight excess to a 0.02 M aqueous solution of sodium pentacyanonitrosylferrate (Wako Chemicals). The precipitates obtained were left overnight for aging, collected by filtration, and dried in air. Elemental analysis yields the formula $\text{Ni}[\text{Fe}(\text{CN})_5\text{NO}]\cdot 5.3\text{H}_2\text{O}$ [Anal. Calcd: Fe, 15.8%; Ni, 16.6%; C, 17.0%; N, 23.7%; H, 2.7%. Found: Fe, 15.5%; Ni, 16.2%; C, 16.2%; N, 22.5%; H, 2.5%].

IR and UV-visible absorption spectra were measured at low temperature. A closed-cycle helium refrigerator (Iwatani Plantech Corp.) was used to cool the sample to a definite

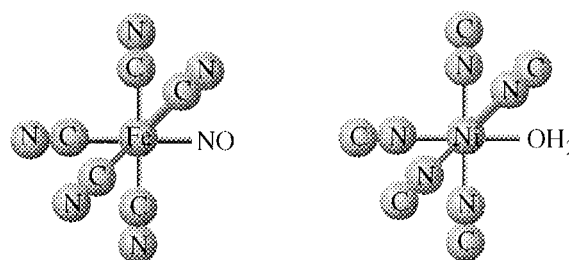


Figure 2. Coordination structures of iron- and nickel-containing moieties.

temperature. IR spectra were obtained with a Bio-RAD spectrophotometer (FTS-40A). The sample was held between CaF_2 plates or ground with KBr and pressed into a disk. UV-visible spectra were recorded on a Shimadzu spectrophotometer (UV-3100PC). For these, the sample was supported on commercial transparent tape. Powder X-ray diffraction was measured at room temperature. Magnetic susceptibilities were measured with a superconducting quantum interference device (SQUID) magnetometer (Quantum Design MPMS-5S). A powder sample for measurement in the SQUID was supported on commercial transparent adhesive tape. An Ar^+ laser (475 nm) was used as the light source, and the blue light was guided by an optical fiber in order to irradiate the sample in the refrigerator and SQUID. The incident intensity was 2 mW/cm^2 .

Results and Discussion

Powder X-ray Diffraction. The powder X-ray diffraction pattern of the nickel nitroprusside corresponds to a face-centered cubic (fcc) structure with a unit-cell parameter of 10.16 \AA . This result coincides with the previous findings.^{24–26} Such a structure was also found in the crystal of cobalt nitroprusside,²⁷ in which coordination of the metal cations was described as follows: each Fe^{II} ion is coordinated by the carbon ends of five CN ligands plus one nitrosyl group, and each Co^{II} ion is coordinated by the nitrogen ends of the CN ligands or by water molecules. CN linkages bridge the metal cations to form a cubic three-dimensional network structure. Same coordination was found in a lot of transition-metal and post-transition-metal nitroprussides.^{27–30} So, it is reasonable to use the same coordination structure for this compound (Figure 2). As the nitroprusside anion has a C_{4v} symmetry, the fcc structure here should be interpreted as an average structure with a local disorder of the water molecules and an arbitrary orientation of the nitrosyl ligand.³¹

IR and UV-Visible Spectra. As the vibrations of the CN and NO ligands are sensitive to the electronic state of the coordinated metal and the coordination environment, they can be utilized as an electronic probe to analyze the coordination and the electronic structure

(24) Gentil, L. A.; Baran, E. J.; Aymonino, P. J. *Inorg. Chim. Acta* **1976**, *20*, 251.

(25) Gentil, L. A.; Baran, E. J.; Aymonino, P. J. *Z. Naturforsch.* **1968**, *23b*, 1264.

(26) Ayers, J. B.; Waggoner, W. H. *J. Inorg. Nucl. Chem.* **1969**, *31*, 2045–2051.

(27) Mullica, D. F.; Tippin, D. B.; Sappenfield, E. L. *J. Coord. Chem.* **1991**, *24*, 83–91.

(28) Mullica, D. F.; Sappenfield, E. L.; Tippin, D. B.; Leschnitzer, D. H. *Inorg. Chim. Acta* **1989**, *164*, 99–103.

(29) Mullica, D. F.; Tippin, D. B.; Sappenfield, E. L. *Inorg. Chim. Acta* **1990**, *174*, 129–135.

(30) Mullica, D. F.; Tippin, D. B.; Sappenfield, E. L. *J. Cryst. Spectrosc. Res.* **1991**, *21*, 81–85.

(31) Reguera, E.; Fernández-Bertrán, J.; Gómez, A. *Eur. J. Solid State Inorg. Chem.* **1994**, *31*, 979–984.

Table 1. Vibration of CN and NO in Ground State (GS) and Metastate (MS)

$\text{Na}_2[\text{Fe}(\text{CN})_5\text{NO}]^a$ GS [cm^{-1}]	$\text{Na}_2[\text{Fe}(\text{CN})_5\text{NO}]^a$ MS [cm^{-1}]	$\text{Ni}[\text{Fe}(\text{CN})_5\text{NO}]^b$ (KBr, GS) [cm^{-1}]	$\text{Ni}[\text{Fe}(\text{CN})_5\text{NO}]^b$ (KBr, MS) [cm^{-1}]	$\text{Ni}[\text{Fe}(\text{CN})_5\text{NO}]^b$ (CaF_2 , GS) [cm^{-1}]	$\text{Ni}[\text{Fe}(\text{CN})_5\text{NO}]^b$ (CaF_2 , MS) [cm^{-1}]	assignment
2175	2167	2202	unknown ^c	2208	unknown ^c	$\nu(\text{C}\equiv\text{N})$
2165	2156	2154		2150		
2161	2152					
2147	2136					
2146	2136					
1954–1942	1834–1835	1949	1821	1952 ^d 1934	1815	$\nu(\text{N}=\text{O})$

^a From Guida, J. A.; Piro, O. E.; Aymonino, P. J. *Solid State Commun.* **1986**, 57, 175–178. ^b Measured at 12 K. ^c Changes are too small to be detected correctly. ^d Appeared as a shoulder.

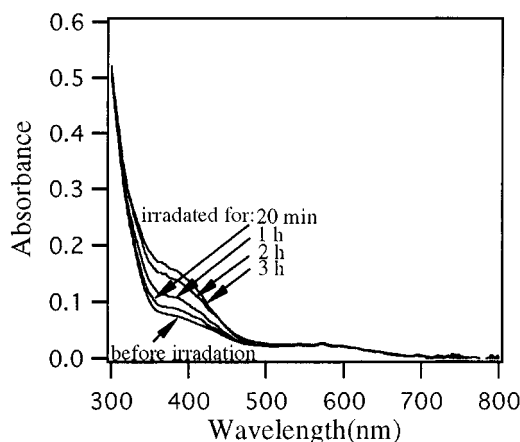


Figure 3. Changes in UV–visible absorption spectra induced by photoirradiation at 12 K.

of the metal cations. In nickel nitroprusside, the infrared spectrum exhibits two CN stretching peaks, ν_{CN} , at higher wavenumbers than those for sodium nitroprusside (Table 1). Such a shift to higher wavenumber for the CN stretch indicates the coordination state of the CN ligand to be $\text{Fe}^{\text{II}}-\text{CN}-\text{Ni}^{\text{II}}$.³² The stretching peak for NO, ν_{NO} , appears at almost the same position as that for sodium nitroprusside, indicating that the electronic state of NO is not significantly changed after the reaction. This may also indicate that the oxygen end of NO does not coordinate to the Ni cation in nickel nitroprusside, which is consistent with the crystal structures of other metal nitroprussides.^{27–30}

The UV–visible absorption spectrum of nitroprusside is shown in Figure 3. The broad band between 490 and 700 nm can be assigned to the d–d transition of nickel.³³ This d–d absorption appears in almost the same wavelength region as that of the aquo complex of nickel. The absorption band existing between 340 and 490 nm as a shoulder can be assigned to the transitions $^1\text{A}_1 \rightarrow ^1\text{E}_1(2b_2 \rightarrow 7e)$, $^1\text{A}_1 \rightarrow ^1\text{A}_1(6e \rightarrow 7e)$, and $^1\text{A}_1 \rightarrow ^1\text{A}_2(2b \rightarrow 3b_1)$ for nitroprusside, in which the $2b_2 \rightarrow 7e$ MLCT transition is believed to appear in the range 441–481 nm.^{33,34} Thus, it can be reasonably expected that irradiation in the 441–481 nm range can induce a MLCT from Fe to NO in the nitroprusside unit. In the case of sodium nitroprusside, potassium nitroprusside, and barium nitroprusside, for example, this MLCT yields a new electronic configuration state which can persist for a long time at low temperature.^{34–36}

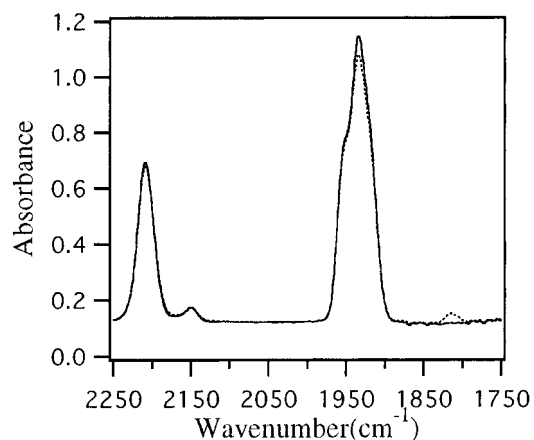


Figure 4. IR spectra before and after irradiation at 12 K (sample is supported by CaF_2 plates). The solid curve is the spectrum before irradiation and the dotted curve is that after irradiation.

A photoinduced spectral change was observed at 12 K. As shown in Figure 3, the photoirradiation caused the absorbance around 400 nm to increase. Figure 4 shows that the IR spectrum of the sample supported between CaF_2 plates exhibits a new peak around 1815 cm^{-1} . In addition, a decrease in intensity of ν_{NO} (1934 cm^{-1}) was observed. All of these changes persist after illumination, and the original state can be restored by a thermal treatment above 200 K. These results are essentially consistent with those observed for metastates in mononuclear compounds of sodium nitroprusside and others, suggesting that the changes observed here are induced by the MLCT from Fe^{II} to the NO group. As the electron is transferred to an NO orbital with antibonding character,³⁴ the NO bond is weakened and ν_{NO} is shifted to a lower wavenumber. No obvious change was observed in ν_{CN} which may be attributed to the small shift of ν_{CN} in metastate just as those in sodium compound (Table 1). The increase of the absorbance in the UV–visible region is also ascribed to a metastate of $\text{Fe}(\text{CN})_5\text{NO}^{2-}$.^{35,37}

From the changes of the ν_{NO} in IR spectrum, the population of metastate, P , can be estimated by

$$P = \frac{A_{\nu_{\text{NO}}}^{\beta} - A_{\nu_{\text{NO}}}^{\alpha}}{A_{\nu_{\text{NO}}}^{\beta}}$$

where $A_{\nu_{\text{NO}}}^{\beta}$ and $A_{\nu_{\text{NO}}}^{\alpha}$ are the areas of ν_{NO} at 1815 cm^{-1}

(32) Nakamoto, K. *Infrared and Raman Spectra of Inorganic and Coordination Compounds*; Wiley-Interscience: New York, 1986.

(33) Inoue, H.; Iwase, H.; Yanagisawa, S. *Inorg. Chim. Acta* **1973**, 7, 259–263.

(34) Manoharan, P. T.; Gray, H. B. *J. Am. Chem. Soc.* **1965**, 87, 3340–3348.

(35) Woike, T.; Krasser, W.; Bechthold, P. S. *Phys. Rev. Lett.* **1984**, 53, 1767–1770.

(36) Pressprich, M. R.; White, M. A.; Vekhter, Y.; Coppens, P. *J. Am. Chem. Soc.* **1994**, 116, 5233–5238.

(37) Krasser, W.; Woike, T.; Haussühl, S.; Kuhl, J.; Breitschwerdt, A. *J. Raman Spectrosc.* **1986**, 17, 83–87.

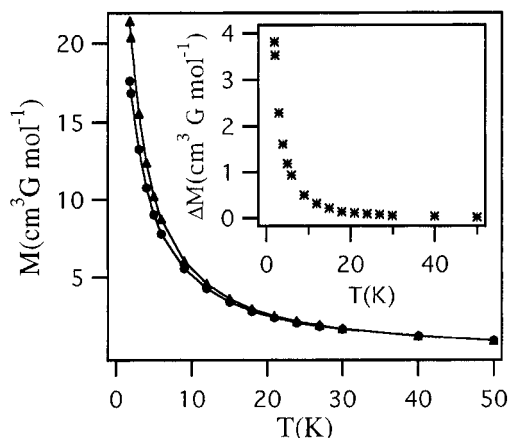


Figure 5. Thermal dependence of magnetization before (●) and after (▲) irradiation. The inset shows the increase of magnetization calculated by $\Delta M = M_a - M_b$, where M_b is the magnetization before irradiation and M_a is that after irradiation.

before and after irradiation, respectively. This calculation shows that the population of the metastate can reach ca. 1.7% after irradiation.

Magnetic Properties. Before irradiation, the effective magnetic moment μ_{eff} at 300 K calculated by the equation $\mu_{\text{eff}} = 2.828(\chi T)$ shows a value of $2.94 \mu_B$ per formula unit of $\text{Ni}[\text{Fe}(\text{CN})_5\text{NO}] \cdot 5.3\text{H}_2\text{O}$, which is slightly larger than the spin-only value $2.83 \mu_B$ at the high-temperature limit for the $\text{Ni}(\text{II})\text{--Fe}(\text{II})$ system, which corresponds to a sum of local contributions from the sites of nickel and iron

$$\mu_{\text{eff}} = (g_{\text{Ni}}^2 S_{\text{Ni}}(S_{\text{Ni}} + 1) + g_{\text{Fe}}^2 S_{\text{Fe}}(S_{\text{Fe}} + 1))^{1/2}$$

where the local Zeeman factors, g_{Ni} and g_{Fe} , are assumed to be 2; and $S_{\text{Ni}} = 1$ and $S_{\text{Fe}} = 0$ are the local spin numbers for Ni and Fe. Because the spin number of $\text{Fe}(\text{II})$ in the low spin state is zero, the interaction between the nearest-neighbor nickel ions is obstructed. No magnetic phase transition can be observed above 1.8 K (Figure 5). A fit of the temperature dependence of the magnetization data to the Curie–Weiss law, $\chi = C/(T - \theta)$, yielded a Weiss constant θ of -0.87 . This small negative value may result from the interaction between Ni^{II} ions. This interaction should be very weak and antiferromagnetic, according to well-known principles.^{18,19} The field dependence of the magnetization can be fitted to an equation of the form $M = g\mu_B S N B_S - (g\mu_B H/kT)$ in which $S = 1$, where μ_B is the Bohr magneton, N is Avogadro's number, k is the Boltzmann constant, and B_S is a Brillouin function (Figure 6). This result agrees with the conclusion derived from the effective moment that there are two spins for one unit of $\text{Ni}[\text{Fe}(\text{CN})_5\text{NO}] \cdot 5.3\text{H}_2\text{O}$.

Photoirradiation of the sample at 5 K induced an immediate increase of the magnetization. As shown in Figure 7, the magnetization at 50 G increased with the illumination time and gradually saturated. The photoenhancement of the magnetization depends significantly on temperature and increases greatly below 20 K (Figure 5). Such temperature dependence indicates the formation of high-spin clusters by photoirradiation.^{38,39} The enhancement of the magnetization can be

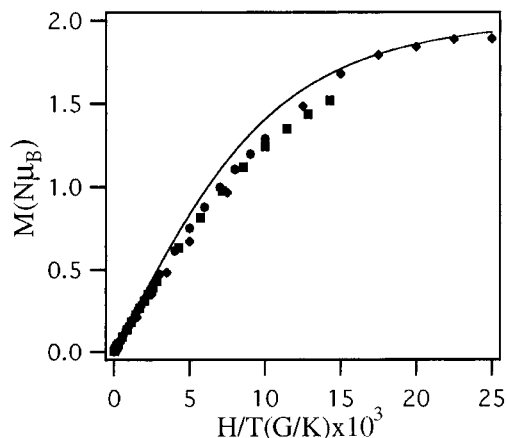


Figure 6. Field dependence of magnetization at 2 K (◆), 3.5 K (■), 5 K (●) which can be fitted to a Brillouin function (solid curve) in which $S = 1$.

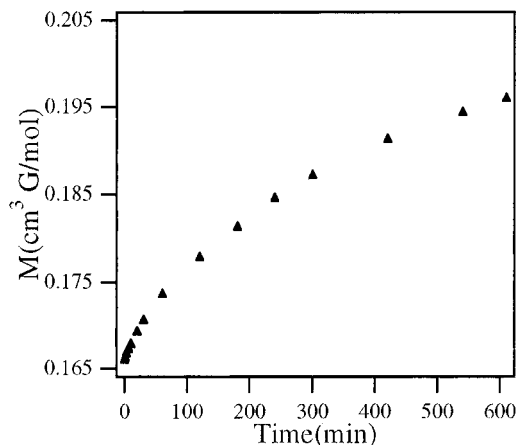


Figure 7. Change of magnetization vs photoirradiation time at 5 K.

induced under 200 K, and all of the changes induced by irradiation can be recovered by thermal treatment at temperatures above 200 K.

Based on the IR and UV–visible absorption spectra induced by photoirradiation, it is concluded that the change in magnetization is caused by the photoinduced MLCT in nitroprusside. In the ground state of nitroprusside, Fe is divalent and there is no net spin ($S = 0$). In this state, there is only a weak antiferromagnetic interaction between the nearest-neighbor nickel cations. The MLCT transfers one electron from Fe to NO, generating spins localized on both Fe ($S_{\text{Fe}} = 1/2$) and NO ($S_{\text{NO}} = 1/2$). Because each Fe is connected to five Ni cations through the CN linkage, which is a good intervening medium for both ferromagnetic and antiferromagnetic interactions, the magnetic coupling between the nearest-neighbor iron and nickel cations appears around the photogenerated trivalent iron with spin, here denoted as Fe^* .

From the changes in the IR spectra, the amount of Fe^* formed compared to the total Fe in the compound was estimated to be only 1.7% at the photostationary state. Therefore it is considered that these Fe^* are dispersed in the material. Only spins on those Ni ions bridged to the Fe^* can be magnetically ordered to form magnetic clusters, which can then produce the enhancement of magnetization after irradiation.

(38) Casan-Pastor, N.; Bas-Serra, J.; Coronado, E.; Pourroy, G.; Baker, L. C. W. *J. Am. Chem. Soc.* **1992**, *114*, 10380–10383.

(39) Caneschi, A.; Ferraro, F.; Gatteschi, D.; Rey, P.; Sessoli, R. *Inorg. Chem.* **1990**, *29*, 4217–4223.

Three types of magnetic clusters can be considered, depending on the exchange interactions between the spins on Ni, NO, and Fe*:

(1) The spin on Fe* couples ferromagnetically with that on NO and antiferromagnetically with that on Ni. In this case, the smallest spin number (S) in a cluster is $S = 4$ (one Fe* is included in each cluster), the second smallest S is 7 (two Fe* are included per cluster), etc.

(2) The spin on Fe* couples antiferromagnetically with that on NO. The smallest S in a cluster is $S = 5$ (one Fe* per cluster), the second smallest S is 9 (two Fe* per cluster), etc. In this case, the spin number of the clusters does not depend on the interaction (ferromagnetic or antiferromagnetic) between Fe* and Ni.

(3) The spin on Fe couples ferromagnetically with those on both NO and Ni. The smallest S is 6 (one Fe* per cluster), the second smallest S is $S = 11$ (two Fe* per cluster), etc.

In general, the magnetization of the clusters M_{clusters} can be calculated as

$$M_{\text{cluster}} = M_1 f_1 + M_2 f_2 + \dots \quad (1)$$

M_1 , M_2 , etc., represent the magnetization of the clusters containing one, two, etc., Fe* atoms, respectively. Similarly, f_1 , f_2 , etc., are the fractions of these clusters.

The magnetization calculated by (1) should be able to be fitted to an expression for the magnetization:

$$M_B = g\mu_B N [S_1 B_{S_1}(g\mu_B H/kT) f_1 + S_2 B_{S_2}(g\mu_B H/kT) f_2 + \dots] \quad (2)$$

$B_S(g\mu_B H/kT)$ is a Brillouin function with spin number S at temperature T .

Because of the low yield of Fe*, it is reasonable to assume that f_1 is much larger than f_i ($i \geq 2$). On the other hand, the difference between M_1 and M_i ($i \geq 2$) is not large, as described above. Thus, it is reasonable to neglect the magnetization resulting from clusters containing more than one Fe*.

In this case, the magnetization of the clusters can be calculated as

$$\begin{aligned} M_{\text{clusters}} &= M_1 \\ &= [M_a - (1 - 5R)M_b]/R \\ &= [\Delta M + 5RM_b]/R \end{aligned} \quad (3)$$

where M_b and M_a are the magnetizations before and after illumination, and the number 5 reflects the number of nickel cations connected to each Fe*. The term $5RM_b$ is the decrease of the paramagnetic portion of in the magnetization due to the formation of magnetic clusters and $(1 - 5R)M_b$ gives the magnetization resulting from Ni cations which do not belong to magnetic clusters after irradiation. R is the mole fraction of Fe* (vs total Fe).

By neglecting the magnetization coming from clusters with more than one Fe*, eq 2 can be rewritten as

$$M_B = g\mu_B S_1 N B_{S_1}(g\mu_B H/kT) \quad (4)$$

By fitting the magnetization derived from eq 3 to eq 4, the spin number per cluster is estimated to be 5. The calculated results also show that the yield of Fe* is 1.9%, which is consistent with the yield (1.7%) derived from

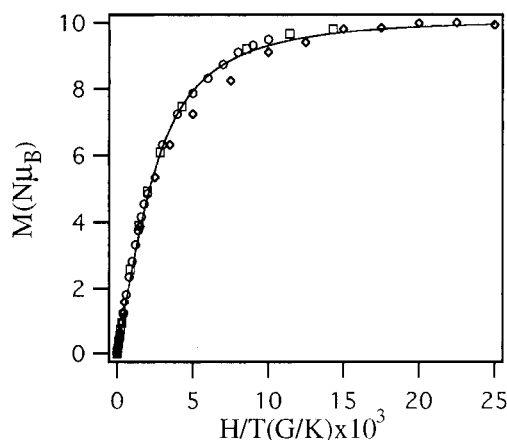


Figure 8. Field dependence of magnetization of photoinduced magnetic clusters at 2 K (\diamond), 3.5 K (\square), 5 K (\circ), which can be fitted to a Brillouin function (solid curve) in which $S = 5$.

IR spectra. As shown in Figure 8, the magnetization of clusters obtained from eq 3 obeys a Brillouin function with $S = 5$. This calculated result indicates that the clusters induced by irradiation belong to type 2, that is, the photogenerated spins on Fe* and NO couple antiferromagnetically.

Because there exists no experimental technique for us to directly determine the interaction between Fe* and Ni^{II}, we analyzed it from the viewpoint of magnetic orbital interactions.^{17,40,41} The overlap of magnetic orbitals centered on different metals is used to analyze the magnetic exchange interaction, that is, when the overlap is zero, the parallel alignment of spins is favored. In this case, the exchange interaction is ferromagnetic. Increasing the overlap decreases the ferromagnetic interaction and causes the antiparallel alignment to become more favored. A large overlap usually contributes a large antiferromagnetic interaction. For nickel nitroprusside, the exchange interaction can be determined from the overlap of the magnetic orbitals of the Fe(CN)₅NO and Ni(NC)₅OH₂ fragments. After irradiation, MLCT induces a spin on the **b**₂ nitroprusside orbital. As shown in Figure 9A, this orbital is mainly composed of the iron d_{xy} and the p_π orbital of the equatorial cyanides. The magnetic orbital for the Ni(NC)₅OH₂ fragment includes two type **a** ($d_{x^2-y^2}$ and d_z^2) orbitals. The d_z^2 type orbital is denoted **a'** to distinguish it from the $d_{x^2-y^2}$ type orbital, denoted **a**. As shown in Figure 9B, the **a** orbital is composed of σ orbitals of equatorial cyanides and the $d_{x^2-y^2}$ orbital of iron, and the **a'** orbital is mainly composed of the iron d_z^2 orbital, σ orbitals of both axial and equatorial cyanides, and the p orbital of O. As the metal cations are linked by a 180° Fe–CN–Ni bridge, the overlap between the **b**₂ orbital and the **a**, **a'** orbitals through the CN linkage is very small. Thus, a ferromagnetic interaction between Fe and Ni is expected. All of these results show that the spins on Ni couple ferromagnetically with that on Fe*, and the spin on NO couples antiferromagnetically with that on Fe* after illumination (Figure 10).

In summary, we have demonstrated a spin switching effect in nickel nitroprusside. Photoirradiation induces

(40) Ginsberg, A. P. *Inorg. Chim. Acta Rev.* **1971**, 5, 45–68.

(41) Klenze, R.; Kanellakopulos, B. *J. Chem. Phys.* **1980**, 72, 5819–5828.

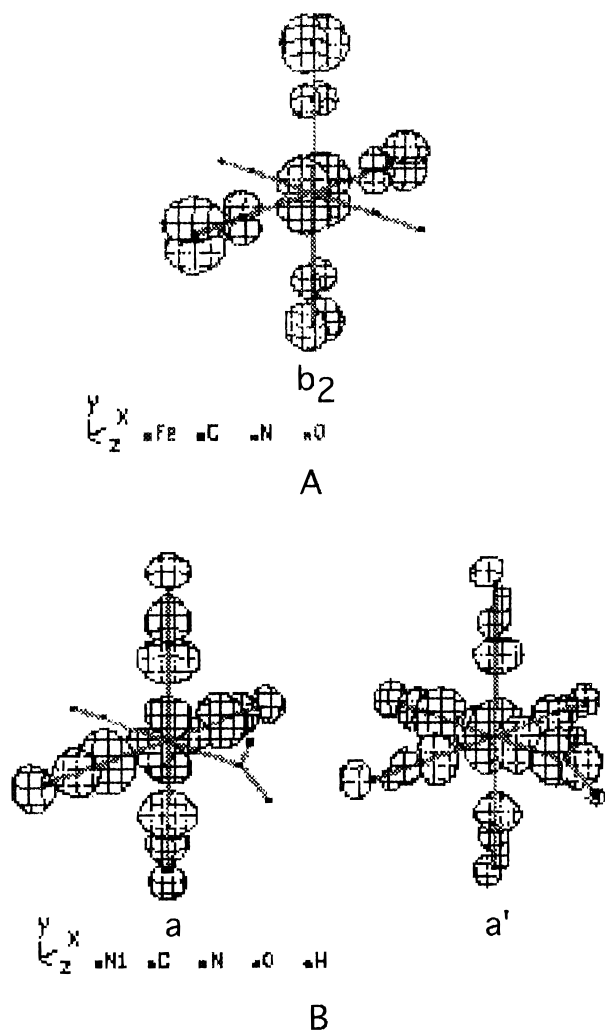


Figure 9. Magnetic orbitals for (A) $\text{Fe}(\text{CN})_5\text{NO}$ and (B) $\text{Ni}(\text{NC})_5\text{OH}_2$ fragments which were calculated using the EHMO method and plotted using the CACAO program.^{44,45}

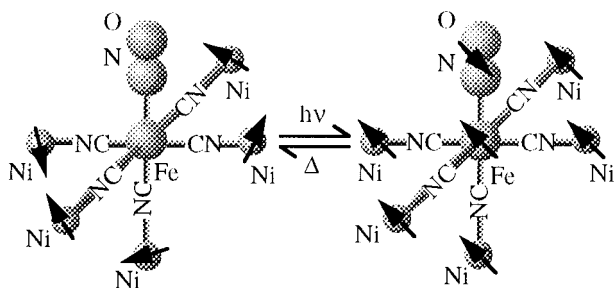


Figure 10. Spins on nickel are randomly oriented around an iron without net spin, while they are ordered around an iron with spin and form a magnetic cluster.

a MLCT from Fe to NO, which produces two antiferromagnetically coupled spins on NO and Fe^* , respectively. The photoinduced spins trigger a strong magnetic coupling between neighboring Ni ions. This compound thus provides a primary model for the construction of the photocontrollable information-transfer devices based

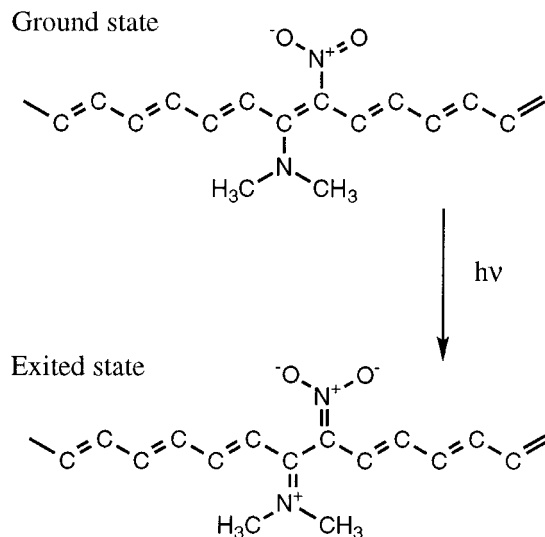


Figure 11. "Soliton switching" model proposed by Carter,⁴² which is constructed by imbedding a push-pull-type olefin in *trans*-polyacetylene. In the ground state, there is a double bond between the two central carbon atoms in the olefin fragment. Thus, the chain of the *trans*-polyacetylene is in a conjugated state. Solitons can be transferred along the chain from one side to the other. In the excited state, the double bond between the two central carbon atoms in the olefin fragment is broken by photoirradiation and becomes a single bond. So, the conjugation is interrupted and the soliton transport is blocked.

on magnetic interactions. The spin acceptor, NO, acts to gate the spin communication between the PMBs through the $-\text{Ni}_i-\text{NC}-\text{Fe}-\text{CN}-\text{Ni}_j-$ linkage. Before irradiation, the spins on the Ni_i and Ni_j ions are unrelated and are thus not coupled. In this state, the information transfer from one PMB to another is blocked by the CCB, which is thus in an off-state. After irradiation, the spins on Ni_i and Ni_j are strongly coupled. In this state, information in the PMBs is transferred through the CCB to each other and thus the CCB is in an on-state. This model is somewhat similar to the "soliton switching" model proposed by Carter⁴² (Figure 11), which provides a simple model for the construction of information devices at the molecular level. However this concept is often regarded as infeasible.⁴³ The spin-based device model proposed in this paper may provide a novel method by which to construct information transfer devices at the molecular level.

Acknowledgment. We thank Dr. D. A. Tryk for carefully reading the manuscript. This work was partially supported by a grant from the Ministry of Education, Science and Culture of Japan.

CM9606383

(42) Carter, F. L. *Molecular Electronic Devices*; Marcel Dekker Inc.: New York, 1982.

(43) Roth, S. *One-Dimensional Metals*; VCH: Weinheim, 1995.

(44) Hoffmann, R. *J. Chem. Phys.* **1963**, *39*, 1397.

(45) Mealli, C.; Proserpio, D. M. *J. Chem. Educ.* **1990**, *67*, 399–402.